TGFβ inducible early gene-1 knockout mice display defects in bone strength and microarchitecture

Sabine Bensamoun, John Hawse, Malayannan Subramaniam, Brice Ilharreborde, Armelle Bassillais, Claude Benhamou, Daniel Fraser, Merry Oursler, Peter Amadio, Kai-Nan An, et al.

TGFβ inducible early gene-1 knockout mice display defects in bone strength and microarchitecture

Sabine F. Bensamoun [a], John R. Hawse [b], Malayannan Subramaniam [b], Brice Ilharreborde [a], Armelle Bassillais [c], Claude L. Benhamou [c], Daniel G. Fraser [d], Merry J. Oursler [d], Peter C. Amadio [a], Kai-Nan An [a], Thomas C. Spelsberg [b],*

[a] Department of Orthopedic Research, Mayo Clinic College of Medicine, 200 First Street SW, Rochester, MN 55905, USA

[b] Department of Biochemistry and Molecular Biology, Mayo Clinic College of Medicine, 200 First Street SW, Rochester, MN 55905, USA

[c] Inserm U 658, CTI (Caracterisation du tissu osseux par imagerie), Orleans, France

[d] Endocrinology, Mayo Clinic College of Medicine, 200 First Street SW, Rochester, MN 55905, USA

Corresponding author:

Thomas C. Spelsberg, PhD
Department of Biochemistry and Molecular Biology
Mayo Clinic College of Medicine,
200 First Street SW
Rochester, MN 55905, USA

Fax: +1 507 284 2053.
E-mail address: Spelsberg.thomas@mayo.edu

ABSTRACT

TGFβ inducible early gene-1 (TIEG) is a member of the Sp/Krüppel-like transcription factor family originally cloned from human osteoblasts. We have previously demonstrated that TIEG plays a role in the expression of important osteoblast marker genes and in the maturation/ differentiation of osteoblasts. To elucidate the function of TIEG in skeletal development and maintenance, we have generated a TIEG knockout (KO) mouse. Three-point bending tests demonstrated that the femurs of TIEG KO mice are significantly weaker than those of wild-type animals. pQCT analysis of tibias revealed significant decreases in bone content, density and size in KO animals compared to wild-type mice. Micro-CT analysis of the femoral head and vertebrae revealed increases in femoral head trabecular separation and decreases in cortical bone thickness and vertebral bone volume in KO mice relative to wild-type controls. In addition, electron microscopy indicated a significant decrease in osteocyte number in the femurs of KO mice. Taken together, these data demonstrate that the bones of TIEG KO mice display an osteopenic phenotype with significantly weaker bones and reduced amounts of cortical and trabecular bone. In summary, an important role for TIEG in skeletal development and/or homeostasis is indicated.

Keywords: TIEG; Osteoblast; TGFβ; Bone; Osteopenia

INTRODUCTION

The TGFβs constitute a family of multifunctional proteins with a wide range of biological activities [38]. TGFβ has been shown to be an important autocrine and paracrine factor in the formation and maintenance of a healthy skeleton. In fact, bone contains some of the highest concentrations of TGFβ with nearly 100 times more than the amount found in either the kidney or the placenta [41]. Although the exact mechanisms of TGFβ action in bone are not yet fully understood, members of this family have been implicated in bone metabolism at several levels [7].

In vivo animal studies have demonstrated that TGFβ is involved in osteogenesis and chondrogenesis and regulates bone growth, cell proliferation and differentiation in chondrocytes and osteoblast (OB) cells [11,19,25]. The expression of dominant-negative TGFβ receptors in OB cells *in vivo* causes a decreased osteocyte density and decreased bone turnover, suggesting that TGFβ regulates OB differentiation [18]. Importantly, studies by Derynck and co-workers [15,16], using transgenic mice, have shown that the over-expression of TGFβ induces an age-dependent loss of bone mass that resembles osteoporosis, caused by increased bone remodeling, whereby the induced bone resorbing osteoclastic activity exceeds the elevated bone formation.

TGFβ has multiple effects on bone cells in culture. Several laboratories, including ours, have shown that OB cells synthesize TGFβ [14,35,36,40,49]. In rodent and human OBs, TGFβ is involved in the regulation of proliferation and differentiation of OB progenitor cells, the regulation of proliferation of mature OB cells at the G1 phase of the cell cycle without any effects on non-proliferating OB cells and, finally, the regulation of bone matrix production and mineralization [5–7].

TGFβ exerts its effects by binding to specific type II serine/ threonine kinase receptors, which in turn initiate intracellular signaling and gene regulation via phosphorylating the type I kinase receptor [22,31]. One of the main pathways affected by TGFβ is the Smad signaling pathway. There are three categories of Smad proteins, the receptor-regulated Smads (R-Smads), common mediator Smad (SMAD 4) and inhibitory Smads (I-Smads). The type I receptor phosphorylates the receptor- associated subclass of Smads 1, 5 and 8 (for BMP) or 2 and 3 (for TGFβ or activin) causing an activation of these Smads and a heterodimerization with Smad 4. These complexes then translocate to the nucleus and bind to the palindromic sequence GTCTAGAC as well as variations in this sequence to regulate target gene expression [22,31].

TGFβ inducible early gene-1 (TIEG) was first discovered in our laboratory as a transcript that is rapidly and transiently induced within 60 min of TGFβ, BMP or EGF treatment of human osteoblasts [44]. It was subsequently found in pancreatic, hepatic and lung epithelial cells, muscle and heart cells, as well as breast and pancreatic carcinomas [4,8,21,37,47,48]. TIEG is a member of the Sp/Krüppel-like factor (KLF) family of three zinc-finger proteins, which are involved in anti- proliferative and apoptosis inducing functions similar to TGFβ action [10]. These factors bind to the GC rich elements via their zinc fingers to regulate target genes involved in cell growth differentiation and apoptosis [9,28,54].

The TIEG gene encodes a 480 amino acid (72 kDa) protein of which the N-terminal region represents the activation domain, the middle region, the repressor domain and the C-terminal region, the DNA binding domain [9,44]. The C-terminal zinc finger region and repression domains of TIEG have more than 90% homology to Sp-1-like transcription factor family members, including TIEG2 and TIEG3 [47,52]. However, the N-terminal domain of TIEG is largely non-homologous.

Our laboratory has also studied the role of TIEG in the TGFβ-Smad signaling pathway. We have demonstrated that TIEG binds to the GC rich/Sp1-like element and positively or negatively

regulates gene transcription [23,24]. We have shown that over-expression of TIEG mimics the effects of TGFβ in human cancer cells, including osteosarcoma [21,47]. As a gene enhancer/activator, TIEG over-expression has been shown to enhance the TGFβ induction of both the Smad binding element reporter gene activity as well as the transcription of the endogenous genes p21, PAI-1 and Smad 2 [23]. The ability of TIEG to enhance TGFβ actions on the Smad pathway was shown to be Smad-dependent because TIEG had no effect on Smad binding element transcription in the absence of Smad4 expression or when an inhibitory Smad protein, Smad7, was over-expressed [23,24].

Our laboratory has previously developed a TIEG KO mouse model. Analysis of these animals has revealed that TIEG KO mice have an increase in the number of osteoblasts present in bone with no concomitant increase in bone formation parameters [43]. Specifically, osteogenic cell cultures derived from the calvaria of TIEG KO mice have decreased expression of important osteoblast marker genes including alkaline phosphatase, osterix and osteocalcin, and these cells also exhibit decreased rates of mineralization in culture. Based on these data, it was of interest to determine the impact that loss of TIEG expression has on the skeleton *in vivo*.

MATERIALS AND METHODS

Animals

TIEG-deficient embryonic stem cells were developed in collaboration with Incyte Genomics (St. Louis, MO) by targeted disruption of 2.3 kb of the TIEG promoter and 5′-flanking sequences, including exon-1, exon-2 and a portion of exon-3. Mice homozygous for this disruption failed to express TIEG mRNA and protein [43]. A total of sixty-four C57Black/129 female mice were utilized for these studies. Seven wild-type (average weight= 15.7 ± 1.3 g) and 7 KO (average weight= 15.6 ± 1.4 g) 3-month-old mice were used for the mechanical testing, micro-CT and electron microscopy studies. Twenty-five wild-type (average weight= 21.8 ± 1.5 g) and 25 KO (average weight= 21.1 ± 1.2 g) 4-month-old mice were used for the pQCT measurements. All mice were housed in a temperature controlled room (22 ± 2°C) with a daily light/dark cycle of 12 h. All animals had free access to water and were fed standard laboratory chow (Laboratory Rodent Diet 5001; PMI Feeds, Richmond, VA). In order to reduce variability, wild-type and KO littermates were used for all experiments performed in the present report. The Institutional Animal Care and Use Committee (IACUC) approved all animal procedures.

Mechanical testing

A three-point bending test was performed on the left femurs of 7 wild-type and 7 TIEG KO mice at the age of 3 months old. Mice were sacrificed using CO2 and the femurs were dissected out of each individual and cleaned to be free of all muscle, tendons and ligaments. The femurs were placed in the anteroposterior direction and disposed on a metal support. This support was composed of 2 borders that were 5 mm apart [51]. The load was applied in the middle of the

femoral shaft with a material testing machine (490.05C, MTS Corp., Minneapolis, MN, USA) at a velocity of 0.3 mm/s. The load displacement curves were recorded and the ultimate force (Fu), stiffness (S) and work to failure (U) were measured [50] for each individual femur.

Peripheral quantitative computed tomography (pQCT)

pQCT measurements were performed with 25 wild-type and 25 TIEG KO mice at the age of 4 months. Mice were placed in a supine position on a gantry using the Stratec XCT Research SA Plus using software version 5.40 (Norland Medical systems, Fort Atkinson, WI). Slice images were measured at 1.9 mm (corresponding to the proximal tibial metaphysis) and at 9 mm (corresponding to the diaphysis of the tibia) from the proximal end of the tibia as previously described [46].

Microcomputed tomography (micro-CT)

Image acquisition

The right femurs (7 wild-type and 7 KO) and L5 vertebrae (7 wild-type and 7 KO) were removed. The bones were scanned using a Skyscan® 1072 micro-CT machine (Skyscan 1072; Skyscan; Aartselaar, Belgium) with a micro-X-Ray source (80 kV, 100 μA, filtered with a 1-mm thick aluminum filter). The transmitted X-ray beam was recorded by a scintillator coupled to a 1024 × 1024 pixels 12-bit digital cooled CCD camera. The radiographic projections were acquired at 70 kV, 100 μA with a fixed exposure time of 3 s per frame and two averaging frames to improve signal to noise ratio. Transmission X-ray images were acquired with a rotation step of 0.45° leading to 400 views over 180 degrees of rotation. The pixel size was isotropic and fixed at 6.25 μm. After scanning, slices were reconstructed with the manufacturer reconstruction software based on Feldkamp algorithm.

Image processing

The trabecular bone was quantified in the vertebral body (160 slices), lower part of the diaphysis (300 slices) and inside the femoral head. One transverse slice, corresponding to the largest diameter of the femoral head, was used for this particular region of bone. The bone volumes were binarized using a unique threshold, which represents the middle between the peak corresponding to trabecular bone and the peak corresponding to background.

Image analysis

Morphological parameters characterizing trabecular bone were derived by using Skyscan software CTan® (Skyscan 1072; Skyscan; Aartselaar, Belgium). The bone volume (BV/TV, %), trabeculae number (TbN, mm), trabecular surface (BS, mm2), trabecular thickness (TbTh, μm) and trabecular spacing (TbSp, μm) were determined. The middle of the diaphysis was used to measure cortical bone parameters. The cortical area, cortical thickness, anterior/posterior (AP) diameter, medial/lateral (ML) diameter and the bending moment were determined as previously described [17].

Transmission electron microscopy (T.E.M)

Fixation, decalcification and processing of bone samples for TEM

The left femur of 6 wild-type and 6 TIEG KO mice were sectioned (2 mm slices). Samples were immediately placed into fixative [(2% (v/v) glutaralde- hyde, 4% (v/v) paraformaldehyde in 0.05 M cacodylate buffer at pH 7.4, with 0.7% (v/v) ruthenium hexamine trichloride (RHT)], (Polysciences, Inc., Warrington, PA.) for 24 h. Fixation, decalcification and embedding of each section were performed using a PELCO BioWave 34700 laboratory microwave (Ted Pella, Inc., Redding, CA). Samples were placed into fresh resin and then polymerized in a 65°C oven

as previously described [30,53]. Ultrathin (0.1 μm) sections were stained with 2% (w/v) uranyl acetate and lead citrate. Micrographs depicting the osteocytes were taken around each femoral cross section. All images were acquired with a Technai G2 12 TEM equipped with an AMT CCD camera, operating at 80 kV at a magnification of 560x.

Statistical analysis (t test)

Unpaired t tests were performed with the software Statgraphics 5.0 (Sigma Plus, Maryland, USA) to compare the mechanical and morphological parameters between the wild-type and TIEG KO mice.

RESULTS

Mechanical testing

Following the development of our TIEG KO mouse model, we first determined whether or not mechanical differences existed in the skeletons of these animals relative to wild-type littermates. As a first step, we performed a three-point bending test on the left femur of 7 wild-type and 7 TIEG KO mice at the age of 3 months. The ultimate force, represented as the peak force (Fu) and reflective of the strength of the bone, as well as the work to failure, represented as the area under the curve (U) and reflective of the energy necessary to result in a fracture, was significantly decreased in TIEG KO mice. Overall, these data demonstrate that the bones of TIEG KO mice are weaker than those of wild-type individuals (Fig. 1 and Table 1). No differences were detected in the stiffness of the bone, which is represented by the slope of the linear portion of the curve (Fig. 1 and Table 1).

pQCT analysis of wild-type and TIEG KO mouse tibias

Based on the fact that TIEG KO mice have weaker bones relative to their wild-type littermates, it was of interest to determine if significant differences existed in specific bone parameters using pQCT. For these studies, the left tibias of 25 wild-type and 25 KO mice were utilized and the data are outlined in Tables 2 and 3. Interestingly, significant decreases in the total mineral content, total bone density, total area, cortical content, cortical area, cortical thickness, periosteal circumfe- rence and endocortical circumference were observed in the tibias of TIEG KO mice in the diaphyseal region (Table 2). Significant decreases were also observed in the metaphyseal region of the tibia and include total mineral content, total bone density, cortical

content, cortical density, cortical area and cortical thickness (Table 3). The percent decrease for each of these parameters ranged from 3.2% to 18.5% (Tables 2 and 3). These data clearly indicate that a significant bone phenotype exists in TIEG KO mice.

Micro-CT analysis of wild-type and TIEG KO mouse femurs and vertebrae

To evaluate differences in bone structure, we performed micro-CT analyses on the L5 vertebrae and femur of 7 wild-type and 7 TIEG KO mice. This analysis revealed significant decreases in trabecular bone volume (BV/TV) and trabecular spacing (Tb.Sp) within the femoral head (Table 4) and significant decrease in trabecular bone volume (BV/TV), surface of trabecular bone (BS) and trabecular thickness (Tb.Th) within the distal diaphysis of the femur (Fig. 2) in TIEG KO mice relative to wild-type littermates. Trends of decreases in the trabecular bone surface density (BS/TV), trabecular thickness (Tb.Th) and number of trabeculae (Tb.N) were observed in the femoral head (Table 4), whereas trends of decreases in the number of trabeculae (Tb.N) and trabecular bone surface density (BS/TV) as well as increases in the trabecular spacing (Tb.Sp) were observed in the distal diaphysis of the femur (Fig. 2) of TIEG KO mice. A significant decrease in the trabecular thickness (Tb.Th) was observed in the L5 vertebrae of TIEG KO mice whereas trends of decreased trabecular bone volume (BV/TV), number of trabeculae (Tb.N), trabecular bone surface (BS), trabecular bone surface density (BS/TV) and increased trabecular spacing (Tb.Sp) were detected (Fig. 2). These data are reflected in representative images of the femoral head region and L5 vertebrae from both wild-type and TIEG KO mice (Fig. 3). Finally, significant decreases were also detected in the cortical area and thickness of the femoral diaphysis of TIEG KO mice (Table 5). In addition trends of decreases in the external diameter (ML), internal diameter (ML), external diameter (AP),

moment of inertia (ML) and moment of inertia (AP) were also observed in this region of the femur in KO animals (Table 5).

Transmission electron microscopy and osteocyte numbers

In light of previous reports demonstrating an increased number of osteoblasts in TIEG KO mice with defects in osteoblast differentiation and mineralization [43], combined with the present data demonstrating a significant bone phenotype in these animals, it was of interest to examine the osteocytes of these individuals. Sections of the left femur of 6 wild-type and 6 KO mice were examined by transmission electron microscopy to determine the number of osteocytes present. Interestingly, analysis of these images revealed that there was a 38% decrease in the density of osteocytes in TIEG KO mice relative to wild-type controls (Fig. 4).

DISCUSSION

Through the morphological and mechanical analysis of TIEG KO mouse bones, we have identified an important role for TIEG in bone development, growth and/or remodeling. Although whole body X-rays of these animals do not reveal any visual differences in their skeletons, mechanical testing, using 3-point bending assays, demonstrated that the femurs of TIEG KO mice are significantly weaker than those of wild-type controls. pQCT analysis of TIEG KO mouse tibias revealed significant decreases in multiple parameters in both the diaphyseal and metaphyseal regions relative to wild-type littermates. Micro-CT analysis of femurs and vertebrae also demonstrated that significant decreases in trabecular bone parameters exist in TIEG KO mice. Interestingly, transmission electron microscopy analyses of these bones revealed that the number of osteocytes is markedly reduced in the KO animals, suggesting that defects in the final stages of osteoblast maturation/differentiation exist and may be responsible for the observed defects in bone morphology and strength. These data correlate well with our previously published data demonstrating that TIEG KO osteoblasts are unable to fully differentiate and mineralize in culture [43]. Collectively, these data demonstrate that deletion of TIEG expression in mice results in a significant bone phenotype resembling osteopenia and implicate an important role for TIEG in the maintenance of bone quality.

TIEG is normally expressed at relatively high levels in bone compared to most other tissues [45]. Following the development of our TIEG KO mouse model, our initial immunohistochemical analysis of tibias isolated from 12-month-old wild-type and TIEG KO animals did not reveal significant differences in a number of specific bone formation/resorption parameters [43].

However, analysis of osteogenic cell cultures isolated from the calvaria of 3-day-old pups revealed significantly reduced expression levels of important osteoblast marker genes includ-

ing alkaline phosphatase, osterix and osteocalcin. Additionally, TIEG KO osteoblasts exhibit reduced rates of mineralization in culture when treated with BMP-2 [43].

Based on these data, we sought to further characterize the bones of younger (3–4 months old) TIEG KO mice. As is demonstrated in the present report, TIEG KO mice, at an age of 3–4 months, display a significant bone phenotype relative to wild-type littermates. Specifically, the long bones of these mice are weaker and reveal significant decreases in multiple ultra structural parameters, in both cortical and trabecular bone, as determined by pQCT and micro-CT analysis. Although the present data do not exactly correlate with our previously reported immunohistochemical studies [43], it is important to note that the previous studies were performed with 12-month- old mice. It is well accepted that compensation for loss of gene expression occurs in many systems including bone and it is possible that a similar phenomenon is occurring in our TIEG KO mice with age.

TIEG is a member of the Sp/Krüppel-like family of transcription factors. Other members of this family have been implicated as playing important roles in bone growth, development and maintenance. Deletion of Sp3 in mice results in lethality immediately after birth; however, detailed examina- tion of embryos revealed severe defects in tooth formation and skeletal ossification [20]. Deletion of osterix, another important member of the Sp/Krüppel-like family of transcription factors, results in the absence of differentiated osteoblasts and no subsequent bone formation [33]. In addition, disruption of the Sp8 gene results in severe truncation of both forelimbs and hindlimbs [3]. Although the bone phenotype described in the present report is not as severe as those reported for other members of the Sp/Krüppel-like transcription factor family, these data nonetheless demonstrate a significant osteopenic phenotype and reveal the importance of TIEG in bone development/growth and/or maintenance.

Interestingly, the deletion of KLF11 (TIEG-2), TIEG's closest family member, does not result in any skeletal, or other, phenotypes observed to date [42]. It is possible that TIEG- 2 is capable

protein functions by binding to the activated receptor complexes which in turn blocks the phosphorylation of R-Smads [2]. In addition, Smad7 can also induce ubiquitin-mediated degradation of active receptor complexes through its ability to recruit E3 ubiquitin ligase family members [2]. The ability of TIEG to repress this inhibitory Smad 7 gene, as well as to increase the expression of Smad2, results in the overall enhancement of Smad signaling in cells. Thus, the loss of TIEG expression would result in the overall suppression of the TGFβ/Smad pathway.

Others have demonstrated that activation of the Smad pathway by TGFβ, specifically Smad 3, results in the inhibition of Runx2, which, in turn, inhibits osteoblast differentiation [1]. Runx2 represents a major osteoblast lineage determining transcription factor involved in directing precursor stem cells to the pre-osteoblast lineage and regulating their subsequent differentiation [26,27]. Runx2 regulates the expression of important osteoblast marker genes including osteocalcin, bone sialo protein, osteopontin and type 1 collagen [12,13,26,27]. Runx2 is also known to induce the expression of osterix, a transcription factor which is required for terminal osteoblast differentiation [33]. It is interesting to note that some of these same genes have decreased expression levels in osteogenic cell cultures isolated from TIEG KO mouse calvaria [43]. It is possible that TIEG, through its regulation of the Smad signaling pathway and the subsequent downstream effects on the expression of important osteoblast marker genes, is also involved in the maturation and differentiation of osteoblasts.

These findings correlate well with the present data demonstrating a significant decrease in the number of osteocytes in TIEG KO mouse bones. The decrease in osteocyte number in TIEG KO mice may reflect defects in osteoblast maturation and differentiation. In addition, previous studies have demonstrated that expression of dominant-negative TGFβ receptors in OB cells in vivo causes a decrease in osteocyte density suggesting a role for TGFβ in OB differentiation [18]. It is possible that deletion of TIEG expression in our knockout mice results in a similar

phenomenon because TIEG is known to mimic the effects of TGFβ [21,47]. Although the exact functions of osteocytes remain to be elucidated, they are believed to work as mechanosensors in bone [34]. Thus, the increased fragility and decreased strength of TIEG KO mouse bones may be caused by the reduced number of osteocytes as has been observed in other model systems [29].

Our data reveal that the lack of TIEG expression results in a significant osteopenic bone phenotype and implicate an important role for TIEG in the maintenance of bone quality. Although the exact mechanisms for this particular bone phenotype are not yet fully understood, it is possible that the overall enhancement of the Smad signaling pathway, and the subsequent down-regulation of important osteoblast marker genes, may in part explain the observed decrease in multiple bone parameters, including bone strength, in our TIEG KO mice.

Acknowledgments

The authors would like to thank Kay Rasmussen for her excellent technical help throughout this study. We would also like to thank Jackie House for her superb secretarial assistance during the course of this study. This work was supported through NIH Grants: DE41053 (TCS), AR52004 (MJO) and DE07352 (JRH), the Mazza Foundation and the Mayo Foundation.

REFERENCES

[1] Alliston T, Choy L, Ducy P, Karsenty G, Derynck R. TGF-beta-induced repression of CBFA1 by Smad3 decreases cbfa1 and osteocalcin expression and inhibits osteoblast differentiation. EMBO J 2001;20:2254–72.

[2] Attisano L, Tuen Lee-Hoeflich S. The Smads. Genome Biol 2001;2 [REVIEWS3010].

[3] Bell SM, Schreiner CM, Waclaw RR, Campbell K, Potter SS, Scott WJ. Sp8 is crucial for limb outgrowth and neuropore closure. Proc Natl Acad Sci U S A 2003;100:12195–200.

[4] Blok LJ, Grossmann ME, Perry JE, Tindall DJ. Characterization of an early growth response gene, which encodes a zinc finger transcription factor, potentially involved in cell cycle regulation. Mol Endocrinol 1995;9:1610–20.

[5] Bonewald LF, Dallas SL. Role of active and latent transforming growth factor beta in bone formation. J Cell Biochem 1994;55:350–7.

[6] Breen EC, Ignotz RA, McCabe L, Stein JL, Stein GS, Lian JB. TGF beta alters growth and differentiation related gene expression in proliferating osteoblasts in vitro, preventing development of the mature bone phenotype. J Cell Physiol 1994;160:323–35.

[7] Centrella M, Horowitz MC, Wozney JM, McCarthy TL. Transforming growth factor-beta gene family members and bone. Endocr Rev 1994;15:27–39.

[8] Chalaux E, Lopez-Rovira T, Rosa JL, Pons G, Boxer LM, Bartrons R, et al. A zinc-finger transcription factor induced by TGF-beta promotes apoptotic cell death in epithelial Mv1Lu cells. FEBS Lett 1999;457:478–82.

[9] Cook T, Gebelein B, Belal M, Mesa K, Urrutia R. Three conserved transcriptional repressor domains are a defining feature of the TIEG subfamily of Sp1-like zinc finger proteins. J Biol Chem 1999;274: 29500–4.

[10] Dang DT, Pevsner J, Yang VW. The biology of the mammalian Krüppel-like family of transcription factors. Int J Biochem Cell Biol 2000;32:1103–21.

[11] D'Souza RN, Litz M. Analysis of tooth development in mice bearing a TGF-beta 1 null mutation. Connect Tissue Res 1995;32:41–6.

[12] Ducy P, Karsenty G. Two distinct osteoblast-specific cis-acting elements control expression of a mouse osteocalcin gene. Mol Cell Biol 1995;15:1858–69.

[13] Ducy P, Zhang R, Geoffroy V, Ridall AL, Karsenty G. Osf2/Cbfa1: a transcriptional activator of osteoblast differentiation. Cell 1997;89:747–54.

[14] Ellingsworth LR, Brennan JE, Fok K, Rosen DM, Bentz H, Piez KA, et al. Antibodies to the N-terminal portion of cartilage-inducing factor A and transforming growth factor beta. Immunohistochemical localization and association with differentiating cells. J Biol Chem 1986;261:12362–7.

[15] Erlebacher A, Derynck R. Increased expression of TGF-beta 2 in osteoblasts results in an osteoporosis-like phenotype. J Cell Biol 1996;132:195–210.

[16] Erlebacher A, Filvaroff EH, Ye JQ, Derynck R. Osteoblastic responses to TGF-beta during bone remodeling. Mol Biol Cell 1998;9:1903–18.

[17] Ferguson VL, Ayers RA, Bateman TA, Simske SJ. Bone development and age-related bone loss in male C57BL/6J mice. Bone 2003;33:387–98.

[18] Filvaroff E, Erlebacher A, Ye J, Gitelman SE, Lotz J, Heillman M, et al. Inhibition of TGF-beta receptor signaling in osteoblasts leads to decreased bone remodeling and increased trabecular bone mass. Development 1999;126:4267–79.

[19] Geiser AG, Zeng QQ, Sato M, Helvering LM, Hirano T, Turner CH. Decreased bone mass and bone elasticity in mice lacking the transforming growth factor-beta1 gene. Bone 1998;23:87–93.

[20] Gollner H, Dani C, Phillips B, Philipsen S, Suske G. Impaired ossification in mice lacking the transcription factor Sp3. Mech Dev 2001;106:77–83.

[21] Hefferan TE, Reinholz GG, Rickard DJ, Johnsen SA, Waters KM, Subramaniam M, et al. Overexpression of a nuclear protein, TIEG, mimics transforming growth factor-beta action in human osteoblast cells. J Biol Chem 2000;275:20255–9.

[22] Heldin CH, Miyazono K, ten Dijke P. TGF-beta signalling from cell membrane to nucleus through SMAD proteins. Nature 1997;390:465–71.

[23] Johnsen SA, Subramaniam M, Janknecht R, Spelsberg TC. TGFbeta inducible early gene enhances TGFbeta/Smad-dependent transcriptional responses. Oncogene 2002;21:5783–90.

[24] Johnsen SA, Subramaniam M, Katagiri T, Janknecht R, Spelsberg TC. Transcriptional regulation of Smad2 is required for enhancement of TGFbeta/Smad signaling by TGFbeta inducible early gene. J Cell Biochem 2002;87:233–41.

[25] Joyce ME, Roberts AB, Sporn MB, Bolander ME. Transforming growth factor-beta and the initiation of chondrogenesis and osteogenesis in the rat femur. J Cell Biol 1990;110:2195–207.

[26] Komori T, Yagi H, Nomura S, Yamaguchi A, Sasaki K, Deguchi K, et al. Targeted disruption of Cbfa1 results in a complete lack of bone formation owing to maturational arrest of osteoblasts. Cell 1997;89:755–64.

[27] Lian JB, Javed A, Zaidi SK, Lengner C, Montecino M, van Wijnen AJ, et al. Regulatory controls for osteoblast growth and differentiation: role of Runx/ Cbfa/AML factors. Crit Rev Eukaryotic Gene Expression 2004;14:1.

[28] Liu C, Calogero A, Ragona G, Adamson E, Mercola D. EGR-1, the reluctant suppression factor: EGR-1 is known to function in the regulation of growth, differentiation, and also has significant tumor suppressor activity and a mechanism involving the induction of TGF-beta1 is postulated to account for this suppressor activity. Crit Rev Oncog 1996;7:101–25.

[29] Liu W, Toyosawa S, Furuichi T, Kanatani N, Yoshida C, Liu Y, et al. Overexpression of Cbfa1 in osteoblasts inhibits osteoblast maturation and causes osteopenia with multiple fractures. J Cell Biol 2001;155:157–66.

[30] Madden V. In: Giberson, Demaree Jr RS, editors. Microwave-Accelerated Decalcification. Microwave Techniques and Protocols. Totowa, NJ: Human Press Inc; 2001.

[31] Massague J. How cells read TGF-beta signals. Nat Rev, Mol Cell Biol 2000;1:169–78.

[32] Massague J. TGF-beta signal transduction. Annu Rev Biochem 1998;67:753–91.

[33] Nakashima K, Zhou X, Kunkel G, Zhang Z, Deng JM, Behringer RR, et al. The novel zinc finger-containing transcription factor osterix is required for osteoblast differentiation and bone formation. Cell 2002;108:17–29.

[34] Nijweide PJ, Burger EH, Klein-Nulend J, Van der Plas A. Principles of Bone Biology. 1st ed. San Diego: Academic Press; 1996. p. 115–26.

[35] Oursler MJ, Cortese C, Keeting P, Anderson MA, Bonde SK, Riggs BL, et al. Modulation of transforming growth factor-beta production in normal human osteoblast-like cells by 17 beta-estradiol and parathyroid hormone. Endocrinology 1991;129:3313–20.

[36] Oursler MJ, Riggs BL, Spelsberg TC. Glucocorticoid-induced activation of latent transforming growth factor-beta by normal human osteoblast-like cells. Endocrinology 1993;133:2187–96.

[37] Ribeiro A, Bronk SF, Roberts PJ, Urrutia R, Gores GJ. The transforming growth factor beta(1)-inducible transcription factor TIEG1, mediates apoptosis through oxidative stress. Hepatology 1999;30:1490–7.

[38] Roberts AB, Spron MB. The transforming growth factor-β. In: Sporn MB, Roberts AB, editors. Peptide Growth Factors and Their Receptors, vol. 1. Berlin: Springer; 1990. p. 419–72.

[39] Robey PG, Young MF, Flanders KC, Roche NS, Kondaiah P, Reddi AH, et al. Osteoblasts synthesize and respond to transforming growth factor- type beta (TGF-beta) in vitro. J Cell Biol 1987;105:457–63.

[40] Schneider HG, Michelangeli VP, Frampton RJ, Grogan JL, Ikeda K, Martin TJ, et al. Transforming growth factor-beta modulates receptor binding of calciotropic hormones and G protein-mediated adenylate cyclase responses in osteoblast-like cells. Endocrinology 1992;131:1383–9.

[41] Seyedin SM, Thomas TC, Thompson AY, Rosen DM, Piez KA. Purification and characterization of two cartilage-inducing factors from bovine demineralized bone. Proc Natl Acad Sci U S A 1985;82: 2267–71.

[42] Song CZ, Gavriilidis G, Asano H, Stamatoyannopoulos G. Functional study of transcription factor KLF11 by targeted gene inactivation. Blood Cells, Mol Dis 2005;34:53–9.

[43] Subramaniam M, Gorny G, Johnsen SA, Monroe DG, Evans GL, Fraser DG, et al. TIEG1 null mouse-derived osteoblasts are defective in mineralization and in support of osteoclast differentiation in vitro. Mol Cell Biol 2005;25:1191–9.

[44] Subramaniam M, Harris SA, Oursler MJ, Rasmussen K, Riggs BL, Spelsberg TC. Identification of a novel TGF-beta-regulated gene encoding a putative zinc finger protein in human osteoblasts. Nucleic Acids Res 1995;23:4907–12.

[45] Subramaniam M, Hefferan TE, Tau K, Peus D, Pittelkow M, Jalal S, et al. Tissue, cell type, and breast cancer stage-specific expression of a TGF-beta inducible early transcription factor gene. J Cell Biochem 1998;68:226–36.

[46] Syed FA, Modder UI, Fraser DG, Spelsberg TC, Rosen CJ, Krust A, et al. Skeletal effects of estrogen are mediated by opposing actions of classical and nonclassical estrogen receptor pathways. J Bone Miner Res 2005;20:1992–2001.

[47] Tachibana I, Imoto M, Adjei PN, Gores GJ, Subramaniam M, Spelsberg TC, et al. Overexpression of the TGFbeta-regulated zinc finger encoding gene, TIEG, induces apoptosis in pancreatic epithelial cells. J Clin Invest 1997;99:2365–74.

[48] Tau KR, Hefferan TE, Waters KM, Robinson JA, Subramaniam M, Riggs BL, et al. Estrogen regulation of a transforming growth factor-beta inducible early gene that

inhibits deoxyribonucleic acid synthesis in human osteoblasts. Endocrinology 1998;139:1346–53.

[49] Tremollieres FA, Strong DD, Baylink DJ, Mohan S. Insulin-like growth factor II and transforming growth factor beta 1 regulate insulin-like growth factor I secretion in mouse bone cells. Acta Endocrinol (Copenh) 1991;125:538–46.

[50] Turner CH, Burr DB. Basic biomechanical measurements of bone: a tutorial. Bone 1993;14:595–608.

[51] Turner CH, Hsieh YF, Muller R, Bouxsein ML, Rosen CJ, McCrann ME, et al. Variation in bone biomechanical properties, microstructure, and density in BXH recombinant inbred mice. J Bone Miner Res 2001;16:206–13.

[52] Wang Z, Peters B, Klussmann S, Bender H, Herb A, Krieglstein K. Gene structure and evolution of Tieg3, a new member of the Tieg family of proteins. Gene 2004;325:25–34.

[53] You LD, Weinbaum S, Cowin SC, Schaffler MB. Ultrastructure of the osteocyte process and its pericellular matrix. Anat Rec A Discov Mol Cell Evol Biol 2004;278:505–13.

[54] Zhang JS, Moncrieffe MC, Kaczynski J, Ellenrieder V, Prendergast FG, Urrutia R. A conserved alpha-helical motif mediates the interaction of Sp1-like transcriptional repressors with the corepressor mSin3A. Mol Cell Biol 2001;21:5041–9.

FIGURES

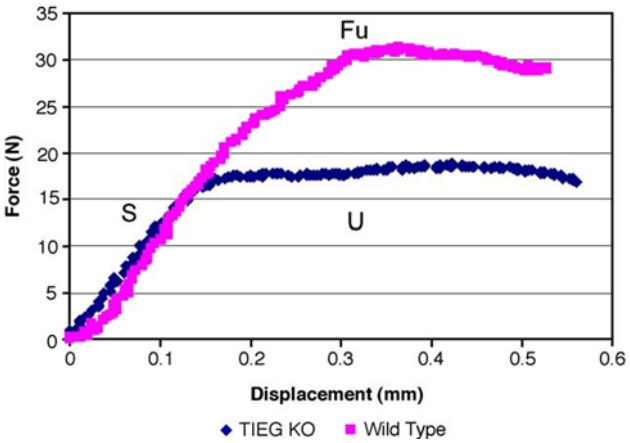

Fig. 1. Graph of 3-point bending test results. Representative force displacement graph generated during a three-point bending test performed on the femurs of 3-month-old wild-type and TIEG KO mice. The ultimate force (Fu), stiffness (S) and work to failure (U) are indicated.

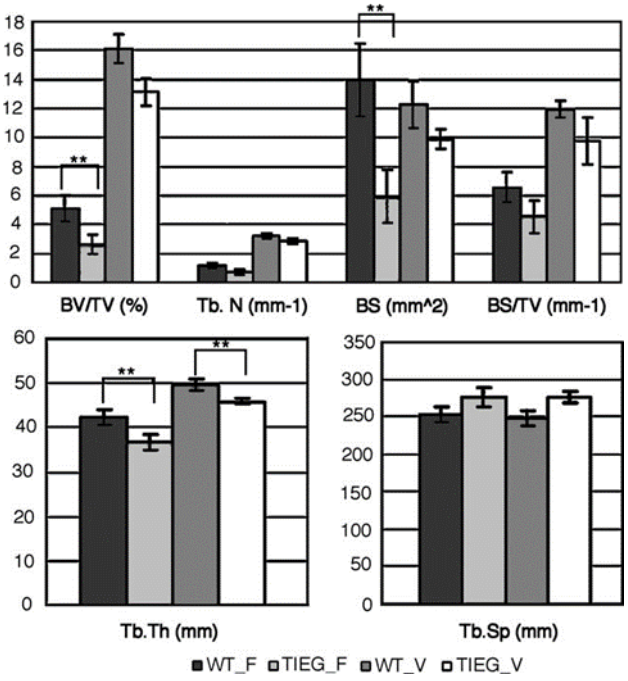

Fig. 2. Graphs depicting trabecular morphological parameters as determined by micro-CT in wild-type and TIEG KO mice. Illustration of the trabecular morphological parameters (mean±SEM) analyzed by micro-CT within the L5 vertebrae (V) and the distal diaphysis of the femur (F) in 3-month-old wild-type (WT) and TIEG KO (TIEG) mice. The following parameters are indicated: trabecular bone volume [BV/TV (%)], number of trabeculae [Tb.N (mm)], surface of trabecular bone [BS (mm2)], bone surface density [BS/TV (mm)], trabecular thickness [Tb.Th (mm)] and trabecular separation [Tb.Sp (mm)]. Significant differences between wild-type and TIEG KO mice are indicated (**P < 0.05).

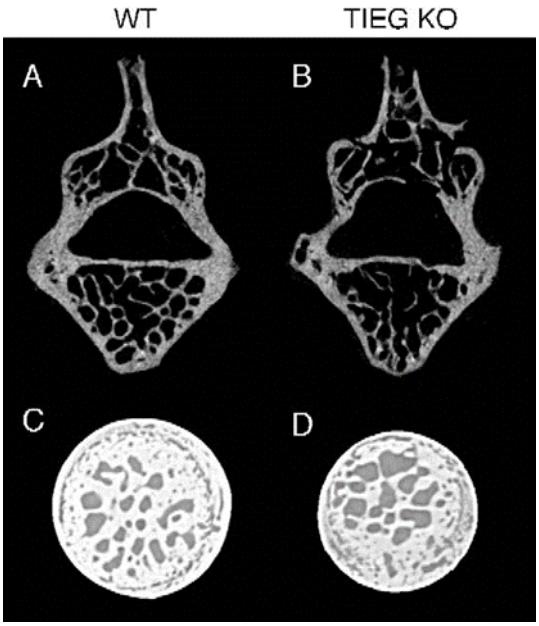

Fig. 3. Representative micro-CT images of the L5 vertebrae and femoral head of wild-type and TIEG KO mice. Representative micro-CT images of the L5 vertebral body of wild-type (A) and TIEG KO (B) mice and the femoral head of wild-type (C) and TIEG KO (D) mice. These images reflect the micro-CT data, graphically represented in Fig. 2, indicating a reduction in multiple trabecular parameters in TIEG KO mouse bones relative to wild-type littermates.

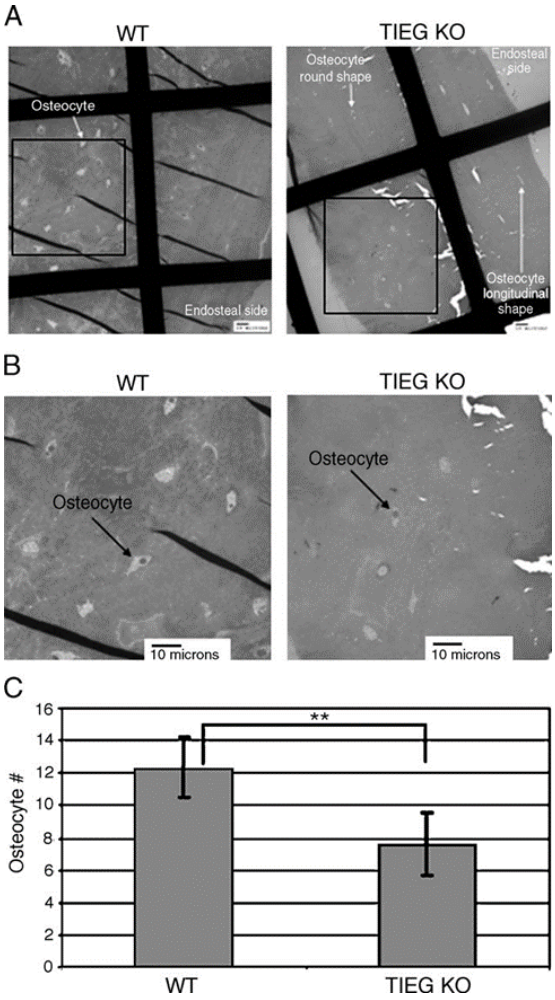

Fig. 4. Electron micrographs and graph depicting reduced numbers of osteocytes in TIEG KO mice. Representative transmission electron microscopy images (560×) (A) and an enlarged image (B) showing the osteocyte cells in the cortical region of the wild-type (WT) and TIEG KO mouse femurs. (C) Graph indicating the average number of osteocytes per 114.28 μm2 in wild-type and TIEG KO mouse femurs (**P < 0.05) as analyzed by transmission electron microscopy.

TABLES

Table 1.

Average ultimate force (Fu), work to failure (U) and stiffness (S) of 7 wild-type and 7 TIEG KO 3-month-old mouse femurs (**P < 0.05) as measured by 3-point bending tests.

	WT	TIEG KO	% Difference
Fu (N)	31.56 ± 1.51	23.31 ± 3.26**	26.1
U (mJ)	10.09 ± 1.11	7.84 ± 1.14**	22.3
S (N/mm)	89.76 ± 8.56	84.41 ± 11.90	6

Table 2.

Morphological parameters (mean±SEM) measured in the tibial diaphysis by pQCT on 4-month-old wild-type (WT) and TIEG KO mice (**P < 0.05)

Tibial diaphysis parameters	WT	TIEG KO	% Difference
Total content (mg)	0.81 ± 0.02	0.73 ± 0.02**	9.9
Total density (mg/cm^3)	674 ± 8.94	638 ± 5.06**	5.3
Total area (mm^2)	1.2 ± 0.02	1.14 ± 0.03**	5
Cortical content (mg)	0.89 ± 0.10	0.79 ± 0.10**	11.2
Cortical area (mm^2)	0.56 ± 0.01	0.50 ± 0.01**	10.7
Cortical thickness (mm)	0.16 ± 0.004	0.15 ± 0.002**	6.3
Periosteal circumference (mm)	4.26 ± 0.24	4.04 ± 0.26**	5.2
Endocortical circumference (mm)	2.88 ± 0.18	2.74 ± 0.22**	4.9

Table 3.

Morphological parameters (mean ± SEM) measured in the tibial metaphysis by pQCT on 4-month-old wild-type (WT) and TIEG KO mice (**P < 0.05)

Tibial diaphysis parameters	WT	TIEG KO	% Difference
Total content (mg)	1.98 ± 0.06	1.75 ± 0.05**	11.6
Total density (mg/cm^3)	581 ± 8.72	555 ± 8.45**	4.5
Cortical content (mg)	1.19 ± 0.04	0.97 ± 0.03**	18.5
Cortical density (mg/cm^3)	942 ± 8.52	912 ± 8.50**	3.2
Cortical area (mm^2)	1.26 ± 0.04	1.06 ± 0.03**	15.9
Cortical thickness (mm)	0.22 ± 0.01	0.19 ± 0.01**	13.6

Table 4.

Trabecular morphological parameters (mean ± SEM) within the femoral head of 3-month-old wild-type (WT) and TIEG KO mice by micro-CT (**P < 0.05)

Femoral head region	WT	TIEG KO	% Difference
BV/TV (%)	56.87 ± 2.81	45.25 ± 2.60**	20.4
BS (mm2)	6.56 ± 0.76	6.80 ± 0.46	3.7
BS/TV (mm)	27.13 ± 1.44	24.21 ± 0.46	10.8
Tb.Th (µm)	74.74 ± 5.05	65.76 ± 2.49	12

Table 5.

Cortical morphological parameters (mean±SEM) measured in the middle of the femoral diaphysis in the mediolateral (ML) and anteroposterior (AP) positions with micro-CT (**P < 0.05) on 3-month-old wild-type (WT) and TIEG KO mice

Cortical parameters	WT	TIEG KO	% Difference
Cortical area (mm^2)	1.00 ± 0.06	0.79 ± 0.05**	21
External diameter ML (mm)	2.01 ± 0.13	1.76 ± 0.08	12.4
Internal diameter ML (mm)	1.23 ± 0.07	1.14 ± 0.04	7.3
External diameter AP (mm)	1.26 ± 0.02	1.24 ± 0.03	1.6
Internal diameter AP (mm)	0.83 ± 0.02	0.87 ± 0.04	4.6
Thickness (µm)	235 ± 10.51	191 ± 15.10**	18.7
Moment of inertia ML (mm^4)	0.16 ± 0.01	0.13 ± 0.02	18.8
Moment of inertia AP (mm^4)	0.43 ± 0.05	0.33 ± 0.06	23.3